Development of CNT/Fe$_2$O$_3$ nanocomposites as electrode materials for advanced supercapacitors

K. Ponnarasi [a,*], P. Elangovan [a], S. Surender [b,c]

[a] PG & Research Department of Physics, Pachaiyappa's College, Chennai, India
[b] School of Engineering, Cardiff University, United Kingdom
[c] Department of Physics, Saveetha School of Engineering, Saveetha Institute of Medical and Technical Sciences (SIMATS), Chennai 602 105, India

ARTICLE INFO

ABSTRACT

Investigating the electrochemical behavior of the CNT/Fe$_2$O$_3$ nanocomposite revealed compelling insights. TEM analysis confirmed the uniform attachment of Fe$_2$O$_3$ nanoparticles to the surface of CNTs. Consequently, in the three-electrode system, the CNT/Fe$_2$O$_3$ nanocomposite hybrid electrode exhibited impressive electrochemical performance. Achieving a high capacitance of approximately 512 F/g at a current density of 1 A/g, the CNT/Fe$_2$O$_3$ nanocomposite electrode showcased a remarkable energy density of 29.5 Wh/kg at a power density of 2.8 kW/kg. The exceptional electrochemical properties of CNT Fe$_2$O$_3$ nanocomposites position them as promising electrode materials for supercapacitors.

1. Introduction

Supercapacitors, recognized as exemplary energy storage devices, have garnered significant interest recently, owing to their impressive attributes such as high-power density, rapid recharge capabilities, and extended cycle life. Nevertheless, the advancement of supercapacitors has been impeded by their limited energy density and low capacitance, posing constraints on their potential for further development in high-performance energy storage devices [1,2]. The profound influence of electrode materials on the electrochemical performance of supercapacitors is well-established. Commonly employed electrode materials encompass transition-metal oxides, carbon, and conducting polymers. While carbon materials exhibit notable cycling stability, they often yield relatively low capacitance. This result is ascribed to the storage mechanism, which involves the creation of a double-layer charge on the electrode's surface. Conversely, the latter two electrode materials frequently present higher capacitance compared to carbon, owing to their storage mechanism that entails redox reactions at the electrode/electrolyte interface [3]. As a consequence, extensive research efforts have been undertaken to explore the potential of transition-metal oxides in enhancing the specific capacitance and energy density of supercapacitors [4]. Iron oxides (Fe$_2$O$_3$) have gotten a lot of interest because of their abundant availability, great theoretical capability, and inexpensive cost [5]. However, Fe$_2$O$_3$, much like numerous other metal

oxides, exhibits weak electrical conductivity, leading to compromised cycling stability and low-rate capability [6,7]. The noted challenge can be addressed by incorporating carbonaceous elements into the composite structure containing Fe2O3. Carbon nanotubes (CNTs), chosen for their outstanding electrical conductivity and unique hollow structure, emerged as a preferable option among various carbon materials [8].

Atomic layer deposition (ALD) [6], atmospheric pressure plasma jets (APPJs) [9], and successive ionic layer adsorption and reaction (SILAR) [2] techniques are some of the ways now used to make Fe$_2$O$_3$/CNTs composite [10]. However, the procedures mentioned earlier entail substantial equipment requirements and high costs, prompting our exploration of a simpler and more cost-effective alternative. In comparison to other methods, both hydrothermal and solution methods are regarded as highly promising for easy scalability to batch-scale production, thanks to their simplicity and economic viability. Herein, with the continuation of our previous work [11], we successfully prepared the different wt. % of CNT/Fe$_2$O$_3$ nanocomposite [12,13] and extended this work towards energy storage application. The hybrid nanocomposite of Fe$_2$O$_3$/CNTs proves to be an excellent performer as a supercapacitor electrode, showcasing outstanding electrochemical performance.

2. Experimental

2.1. Preparation of CNT/Fe₂O₃ nanocomposite

Commercial multi-wall CNTs (20–50 nm in diameter, Sigma Aldrich.) with >95 % purity, 20–30 nm outer diameter, 5–10 nm inner diameter, and 0.5–2.0 μm length were purified by refluxing the required amount of as-received sample in 50 mL nitric acid (HNO_3) with 20 mL sulfuric acid (H_2SO_4) for 10 h. The acid-treated MW-CNTs were then collected thru filtration and dried at 70 °C for 10 h in a vacuum. The detailed preparation method of Fe_2O_3 and Fe_2O_3/CNTs nano composites were described in our previous report [11].

2.2. Materials characterization

The crystalline phases of the prepared samples were scrutinized using X-ray diffraction (XRD) analysis (Bruker AXS D8, Bruker, Germany). The microstructures of the products were studied by scanning electron microscope (SEM, TESCAN, MAIA 3 LMH) and transmission electron microscope (TEM, JEOL, JEM 2100F). The chemical composition and elements present in samples and their corresponding valence states in samples were determined by X-ray photoelectron spectroscopy (XPS, Thermo Fisher, ESCALAB-250).

2.3. Electrochemical measurements

Electrochemical assessments, encompassing cyclic voltammetry (CV), galvanostatic charge/discharge (GCD), and electrochemical impedance spectroscopy (EIS) tests, were conducted using a CHI660e electrochemical workstation from Shanghai Chenhua. The electrochemical properties were evaluated in a 3 M KOH solution as the electrolyte, employing a CHI electrochemical workstation. The analyses were performed in a three-electrode configuration, where CNT/Fe₂O₃ nanocomposite-coated Nickel foam substrates served as the working electrode, platinum functioned as the counter electrode, and Ag/AgCl served as the reference electrode.

For the preparation of the working electrode, a mixture of active material (CNT/Fe₂O₃ nanocomposite), carbon black, and PVDF in a weight ratio of 80:10:10 was combined with N-methylpyrrolidone (NMP) as the solvent. This resulting mixture was then coated onto a Nickel foam substrate (1 cm/1 cm) and dried at 80 °C in an oven for 12 h. The weight of the active material in the working electrode was measured to be approximately 1 mg. Based on the GCD curves, the specific capacitance (C: F/g), energy density (E: Wh/kg) and power density (P: kW/kg) of supercapacitors were calculated from equations below [2]

$$C = 4*I*\Delta t/m*V \tag{1}$$

$$E = CV^2/7.2 \tag{2}$$

$$P = 3.6*E/\Delta t \tag{3}$$

Where, Δt is the discharge time (s), I is the discharge current (A), m is the mass loading (g) of the material on nickel foam and ΔV Potential window.

3. Results and discussion

It is well known that the iron oxides can crystallize in several altered structures with various proportions of Fe ions of Fe^{2+} and Fe^{3+}. However, the most stable and renowned structures of iron oxides remain FeO, Fe_2O_3, and Fe_3O_4. The XRD patterns of bare Fe_2O_3 and 5 & 10 wt% CNT/Fe₂O₃ composites are shown in Fig. 1. Interestingly, all diffraction peaks are assigned for α-Fe₂O₃ (JCPDS NO.33-0664). XRD confirms all three sample have Fe_2O_3 phase and for 10 wt%CNT/Fe₂O₃ sample
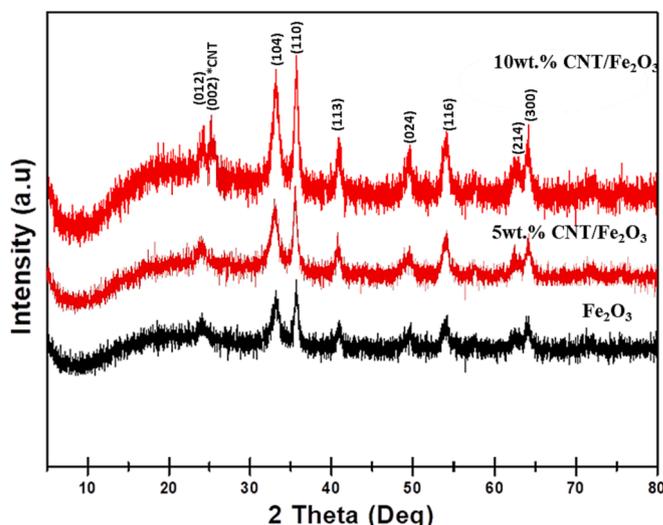
Fig. 1. XRD patterns of Fe₂O₃, 5 and 10 wt% CNT/Fe2O3 nanocomposite.

additionally (0 0 2) plane of carbon was observed. And the average crystallite sizes of pure Fe_2O_3 particles and CNT/Fe₂O₃ nanocomposite were calculated by the Scherrer Formula are about 20–35 nm.

The surface morphology of the nanocomposites were investigated by FE-SEM and TEM analysis as shown in Fig. 2. Notably, Fig. 2(a-b) and (c-d) showing the FE-SEM images of bare Fe_2O_3 and 5 wt% CNT/Fe₂O₃. It is showing that the Fe_2O_3 particles have an average diameter of ~50 nm, and the CNT having a diameter of 30–40 nm. Introducing CNTs into composite can effectively restrain the agglomeration of Fe_2O_3 nanoparticles. Besides, Fig. 2(e) revealing the electron microscopic images of 10 wt% CNT/Fe₂O₃ nanocomposite, the intertwined network of CNTs coated with Fe_2O_3 nanoparticles revealing the high dispersion of Fe_2O_3 with 10 wt%CNT. Moreover, the strong interaction between Fe_2O_3 nanoparticles and CNTs prevented the development of agglomerates of the two components [14]. Further TEM image in Fig. 2(f) shows that Fe_2O_3 nanoparticles were uniformly anchored on the surface of CNTs.

The XPS survey spectrum of bare Fe_2O_3 and 10wt.%CNT/Fe₂O₃ nanocomposite were used to reveal the chemical compositions of the prepared samples and they are shown in Fig. 3. Furthermore, the XPS survey spectrum testifies the existence of C, O, and Fe elements in composite. The major peaks due to the C1s and O1s photoelectrons can be perceived in the scan. For example, the change in the C1s can be attributed to the carbon atoms in the CNTs, however pure Fe_2O_3 also perceived the C1s peak and this may be attributed to the reference carbon paste or tap. For both samples, the major XPS peaks are observed in the binding energy (B.E) range of 705–740 eV and 528–540 eV, which corresponds to the Fe 2p and O 1 s states. Besides, related to Fe 2p peak, less intensity peaks were perceived for Fe 3 s and 3p states. The peak position consistent to Fe 3p, Fe 2p 3/2, 1/2 is respectively around ~55, 710, and 724 eV agreeing very closely to the previously reported [15]. There is also a typical shake-up satellite around ~719 eV. The presence of a peak in BE at 710 eV is assigned to Fe^{3+}. Moreover, as shown in Fig. 3, the Fe2p peaks clearly showing that the presence of iron in bare Fe_2O_3 and 10wt.%CNT/Fe₂O₃ nanocomposite.

In order to evaluate the oxidation and reduction potential CV analysis carried out. The cyclic voltammetry (CV) curves of pure Fe_2O_3 and CNT/Fe₂O₃ were acquired at a scan rate of 100 mV/s in 3 M KOH solution, with the potential range between 0 V and 0.55 V (Fig. 4a). All the CV curves exhibit psedocapacitance behavior along with reduction peak. The GCD profiles of pure Fe_2O_3 and CNT/Fe₂O₃ nanocomposite are shown in Fig. 4b with the same current density of 1 A/g. The discharge time of the CNT/Fe₂O₃ nanocomposite was longer than that of the pure Fe_2O_3, indicating that it has a greater capacitance. According to equation (1), the capacitance of the 10 wt% CNT/Fe₂O₃ electrode was 540 F/
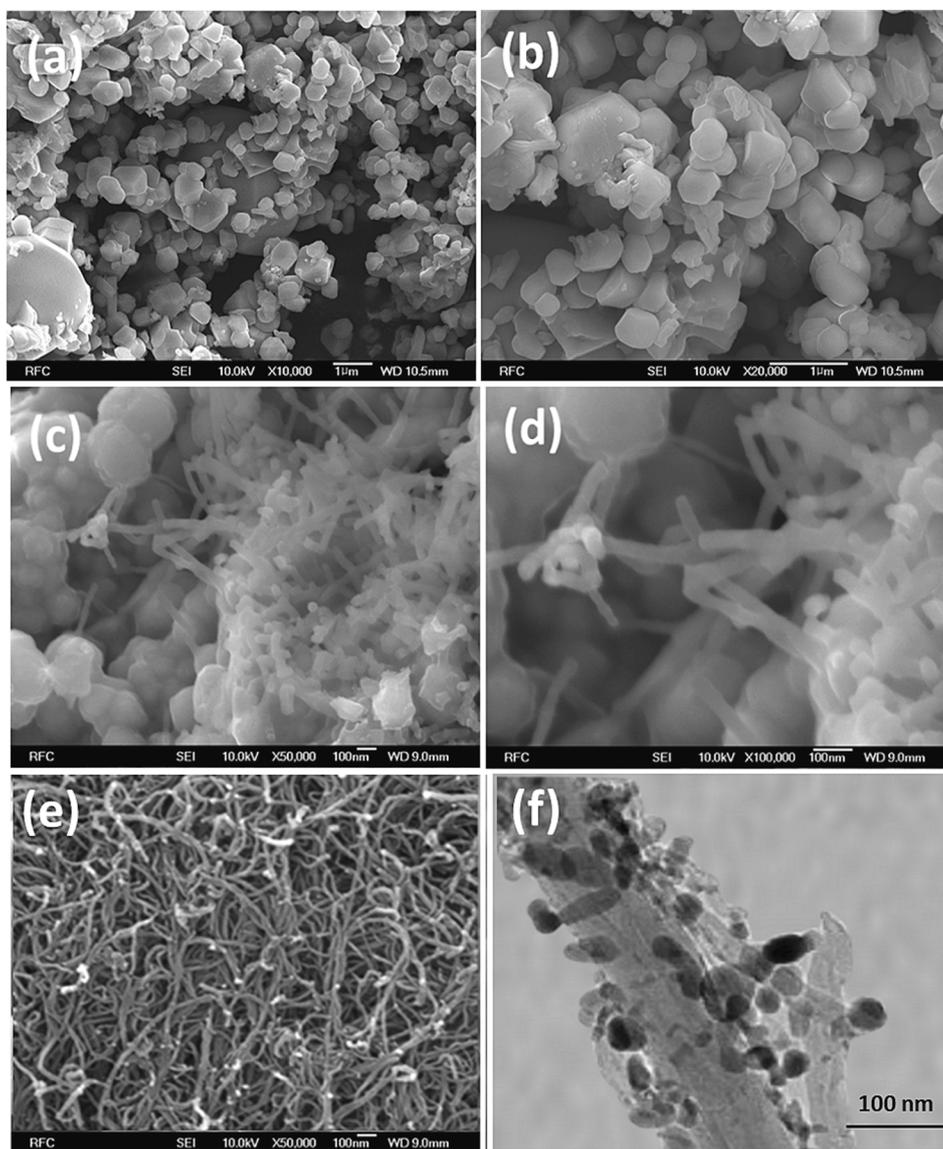
Fig. 2. (a-b) FE-SEM images of pure Fe$_2$O$_3$ particles, (c-d) 5wt.%CNT/Fe$_2$O$_3$ (e) 10wt.%CNT/Fe$_2$O$_3$ and (f) TEM image of 10wt.%CNT/Fe$_2$O$_3$.
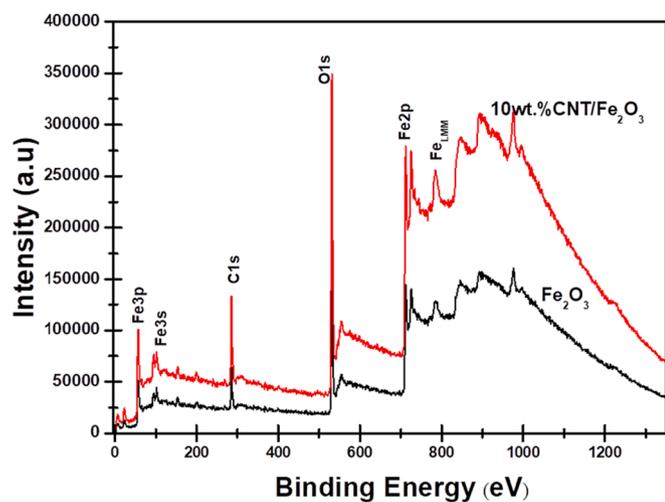
Fig. 3. XPS survey spectra of pure Fe$_2$O$_3$ and 10wt.%CNT/Fe$_2$O$_3$ nanocomposite.

g, while the capacitance of the pure Fe$_2$O$_3$ and 5wt.%CNT/Fe$_2$O$_3$ nanocomposite electrodes were around 120F/g and 232 F/g, respectively. This is because, after adding CNTs to Fe$_2$O$_3$, the composite had increased conductivity and could offer a large number of active sites for a redox reaction to increase capacitance. As stated in Table 1, this finding was also compared to earlier similar publications. The EIS (Fig. 4c) shows that the resistance of the CNT/Fe$_2$O$_3$ nanocomposite hybrid electrodes was lower than that of the pure Fe$_2$O$_3$ electrode. This is due to the ability of the carbon nanotube network and tiny Fe$_2$O$_3$ nanoparticles to shorten the charge transport path [6]. Furthermore, the cycling performances of pure Fe$_2$O$_3$, and CNT/Fe$_2$O$_3$ nanocomposite electrodes were investigated at the same current density of 1 A/g. After 2000 cycles, the capacitance retention rate of the 10 wt% CNT/Fe$_2$O$_3$ electrode was 85.5 % of its initial value. This is due to the CNT/Fe$_2$O$_3$ composite having higher conductivity than bare Fe$_2$O$_3$.

The energy density of 10 wt% CNT/Fe$_2$O$_3$ nanocomposite was 29.5 Wh/kg at 2.8 kW/kg power density, which was greater than bare Fe$_2$O$_3$ and 5 wt% CNT/Fe$_2$O$_3$ (16.1 Wh/kg and 19.7 1 Wh/kg respectively). This finding revealed that the CNT/Fe$_2$O$_3$ combination performed better electrochemically than bare Fe$_2$O$_3$.
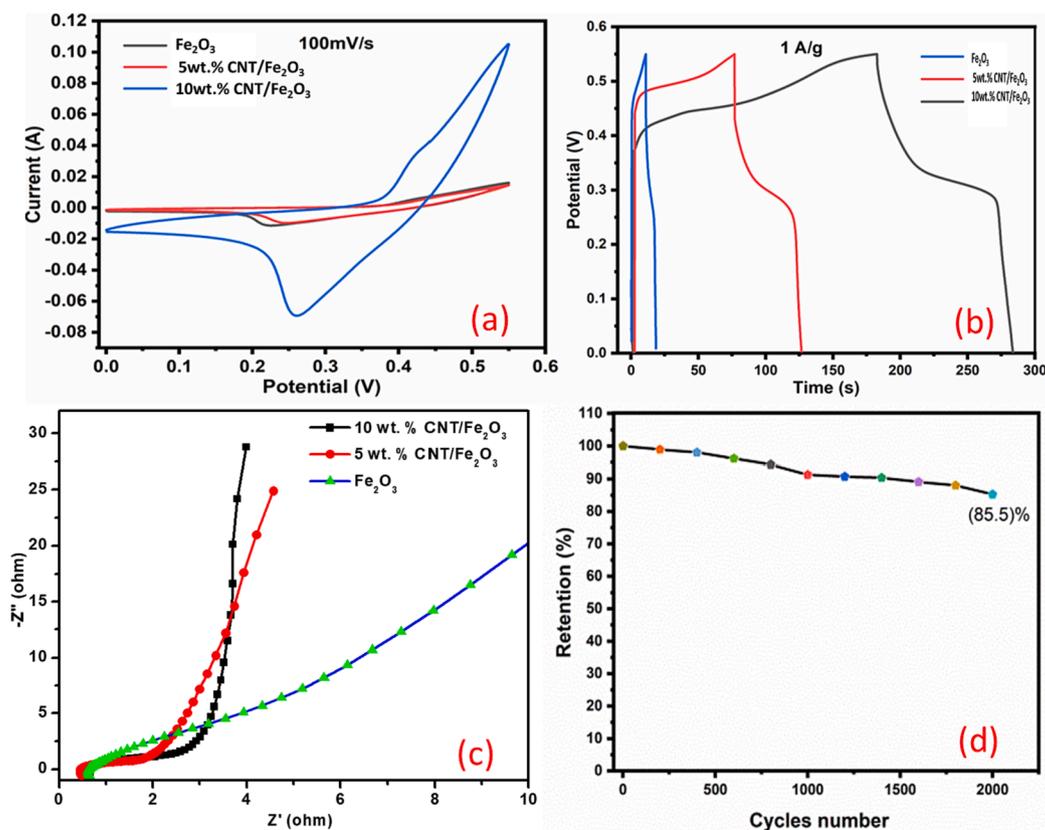
Fig. 4. (a) The CV curves of CNT/Fe$_2$O$_3$ electrode,(b)The GCD curves at current density of 1 A/g, (c) The EIS of Fe$_2$O$_3$ electrode and CNT/Fe2O3 electrode, and (d) Capacitance retention performance 10 wt% CNT/Fe$_2$O$_3$ nanocomposite electrode material.

Table 1
The capacitance reported in recent papers of CNT/Fe2O3 based composite electrodes prepared by various methods.

S. No	Active material	Electrolyte	Capacitance	Reference
1	Fe$_3$O$_4$/CNT	6 M KOH	117.2 at 10 mA cm^{-3}	[16]
2	ά- Fe$_2$O$_3$/MWNT	1 M LiClO4	100 at 5 mV s^{-1}	[17]
3	Fe$_2$O$_3$/MWCNTs	1 M Na2SO3	431 at 5 mV s^{-1}	[2]
4	Nanoporous Fe$_2$O$_3$/CNTs	2 M KCl	54F/g at 2 mV s^{-1}	[9]
5	Fe$_2$O$_3$/CNTs	1 M Na$_2$SO$_4$	204F/g at 0.5 A/g	[18]
6	**5 wt% CNT/Fe$_2$O$_3$**	**3 M KOH**	**232F/g at 1 A/g**	**This Work**
7	**10 wt% CNT/Fe$_2$O$_3$**	**3 M KOH**	**540F/g at 1 A/g**	**This Work**

4. Conclusion

In summary, a hierarchical CNT/Fe$_2$O$_3$ composite was successfully prepared using the hydrothermal approach. The incorporation of CNTs into Fe$_2$O$_3$ significantly enhances the conductivity of the composite material. The CNT/Fe2O3 nanocomposite exhibits exceptional capacitance, high energy density, and remarkable cycling stability, suggesting its potential application in supercapacitors. Moreover, the hydrothermal method provides a straightforward and environmentally friendly pathway for the large-scale fabrication of CNT/Fe$_2$O$_3$ nanocomposites.

CRediT authorship contribution statement

K. Ponnarasi: Conceptualization, Formal analysis, Methodology, Writing – original draft. **P. Elangovan:** Conceptualization, Methodology, Validation, Supervision. **S. Surender :** Conceptualization, Formal analysis, Investigation, Methodology, Supervision, Validation, Writing –

original draft, Writing – review & editing.

Declaration of competing interest

The authors declare that they have no known competing financial interests or personal relationships that could have appeared to influence the work reported in this paper.

Data availability

The data that has been used is confidential.

References

[1] Y. Li, et al., Fe2O3 Nanoneedles on Ultrafine Nickel Nanotube Arrays as Efficient Anode for High-Performance Asymmetric Supercapacitors, Adv. Funct. Mater. 27 (14) (2017).
[2] S.S. Raut, B.R. Sankapal, Comparative studies on MWCNTs, Fe2O3 and Fe2O3/MWCNTs thin films towards supercapacitor application, New J. Chem. 40 (3) (2016) 2619–2627.
[3] S. Sun, et al., Boosted crystalline/amorphous Fe2O3-δ core/shell heterostructure for flexible solid-state pseudocapacitors in large scale, Nano Energy 45 (2018) 390–397.
[4] X. Cheng, et al., Three-dimensional α-Fe2O3/carbon nanotube sponges as flexible supercapacitor electrodes, J. Mater. Chem. A 3 (42) (2015) 20927–20934.
[5] N. Jabeen, et al., High-performance 2.6 V aqueous asymmetric supercapacitors based on in situ formed Na0.5MnO2 nanosheet assembled nanowall arrays, Adv. Mater. 29 (32) (2017).

[6] M. Li, H. He, Study on electrochemical performance of multi-wall carbon nanotubes coated by iron oxide nanoparticles as advanced electrode materials for supercapacitors, Vacuum 143 (2017) 371–379.

[7] Q. Xia, et al., Nanostructured Iron oxide/hydroxide-based electrode materials for supercapacitors, ChemNanoMat 2 (7) (2016) 588–600.

[8] R.M. Kore, B.J. Lokhande, A robust solvent deficient route synthesis of mesoporous Fe2O3 nanoparticles as supercapacitor electrode material with improved capacitive performance, J. Alloy. Compd. 725 (2017) 129–138.

[9] C.H. Xu, et al., Atmospheric pressure plasma jet processed nanoporous Fe2O3/CNT composites for supercapacitor application, J. Alloy. Compd. 676 (2016) 469–473.

[10] F. Yu, et al., Magnetic carbon nanotubes synthesis by Fenton's reagent method and their potential application for removal of azo dye from aqueous solution, J. Colloid Interface Sci. 378 (1) (2012) 175–183.

[11] B. Seenuvasan, P. Elangovan, Synthesis, structural and morphological analysis of carbon nanotube doped α-Fe2O3 hybrid composite prepared by solution method, Mater. Today:. Proc. 68 (2022) 352–355.

[12] P. Huang, et al., N-doped coaxial CNTs@α-Fe2O3@C nanofibers as anode material for high performance lithium ion battery, J. Energy Chem. 27 (5) (2018) 1453–1460.

[13] S. Chandrasekaran, et al., Highly-ordered maghemite/reduced graphene oxide nanocomposites for high-performance photoelectrochemical water splitting, RSC Adv. 5 (37) (2015) 29159–29166.

[14] K. Xie, et al., Highly ordered iron oxide nanotube arrays as electrodes for electrochemical energy storage, Electrochem. Commun. 13 (6) (2011) 657–660.

[15] J. Desai, et al., FT-IR, XPS and PEC characterization of spray deposited hematite thin films, Appl. Surf. Sci. 252 (5) (2005) 1870–1875.

[16] D. Guan, et al., Hydrothermal synthesis of carbon nanotube/cubic Fe3O4 nanocomposite for enhanced performance supercapacitor electrode material, Mater. Sci. Eng. B 178 (10) (2013) 736–743.

[17] X. Zhao, C. Johnston, P.S. Grant, A novel hybrid supercapacitor with a carbon nanotube cathode and an iron oxide/carbon nanotube composite anode, J. Mater. Chem. 19 (46) (2009) 8755–8760.

[18] L. Yue, et al., Microwave-assisted one-pot synthesis of Fe2O3/CNTs composite as supercapacitor electrode materials, J. Alloy. Compd. 765 (2018) 1263–1266.